

## Resonant Dielectronic and Direct Excitation in Crystal Channels

S. Datz, C. R. Vane, P. F. Dittner, J. P. Giese, J. Gomez del Campo, N. L. Jones, H. F. Krause,  
P. D. Miller, M. Schulz, H. Schöne, and T. M. Rosseel

*Oak Ridge National Laboratory, Oak Ridge, Tennessee 37831-6377*

(Received 9 May 1989)

We have observed dielectronic and direct excitation of H-like  $S^{15+}$  and  $Ca^{19+}$  and He-like  $Ti^{20+}$  ions in silicon channels caused by collision with weakly bound target electrons which behave as a free-electron gas. As *in vacuo*, relaxation of the doubly excited states can occur radiatively leading to ions of decreased charge, but in a crystal channel collisional effects can cause double ionization. The effects are seen in both the x-ray yields and charge-state fractions, and, in the case of  $Ti^{20+}$ , in charge-state x-ray coincidences.

PACS numbers: 34.80.Kw, 34.80.Dp, 61.80.Mk

Energetic ions traveling through crystals at small angles to low index directions may be steered to avoid hard collisions ("channeling") and interact in close collisions only with loosely bound electrons. For ion velocities  $v_i \gg v_f$ , where  $v_f$  is a target Fermi-electron velocity representative of the sampled electrons, the penetrating ion may be viewed as being bombarded by a flux of electrons moving at velocity  $v_i$ . The qualitative verity of this approximation was first demonstrated<sup>1</sup> in 1972 when oxygen ions (2 MeV/nucleon) channeled through thin gold crystals were shown to undergo electron capture and loss which could be characterized by interactions with only valence electrons. Since that time, the effect has been used in numerous and varied investigations.<sup>2</sup> Most recently, it has been employed to study radiative electron capture<sup>3</sup> for  $Xe^{54+}$  at 80 MeV/nucleon and to give a measure of the electron impact ionization cross section for  $U^{9+}$  ( $q=88-91$ ) at 405 MeV/nucleon.<sup>4</sup> In these latter two experiments, the target was thin compared to secondary events such as reionization or recapture, respectively, and the energy dependence of the studied processes was assumed to be monotonic and was not studied.

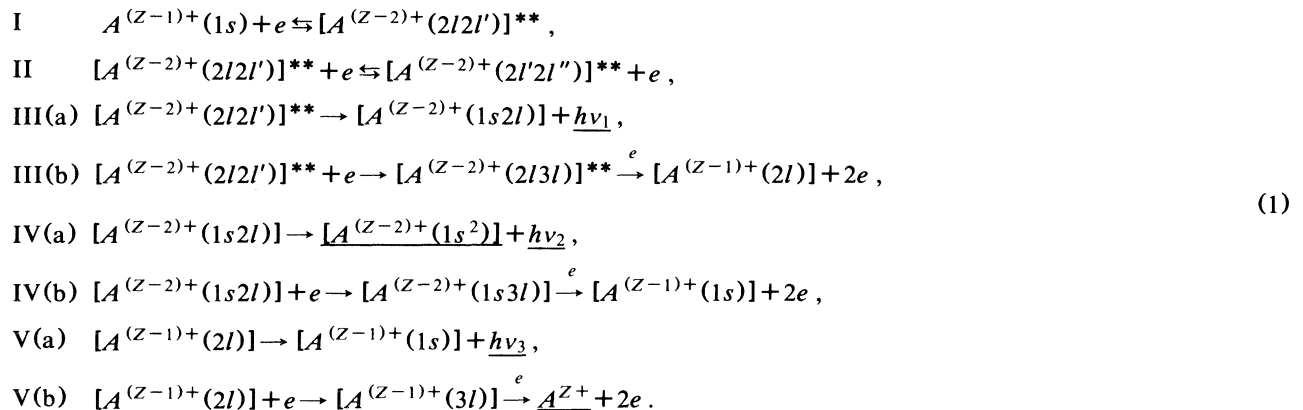
If the assumptions made above are quantitatively correct, ions traveling through this medium at velocities  $v_i$  equivalent to electron velocities required for sharply varying processes, such as dielectronic or direct excitation of an electron bound to the ion, should experience

events similar to those in a hot dense plasma, but with a relatively narrow electron energy distribution, i.e., a Fermi distribution as against a Maxwell-Boltzmann distribution at the temperature necessary to carry out these excitation processes.

In dielectronic excitation, an electron colliding with the ion moving in the channel excites a previously bound electron and, in so doing, loses energy and is captured to a discrete state forming a doubly excited ion. These resonances occur below the energy required for direct excitation. Direct excitation (unlike ionization), rises sharply at its energy threshold. These sharp features will be spread in energy by the Compton profile of the Fermi-electron momentum distribution.

In vacuum under single-collision conditions, the doubly excited state would decay either by an Auger process or by radiative stabilization (dielectronic recombination). In dielectronic recombination, the final result is the production of an ion of reduced charge and two photons. However, if the excited state is created in a dense electron medium (i.e., a dense plasma or a crystal channel), secondary collisional processes leading to further excitation and ionization can come into play and may even dominate.

If we take, as an example, a *KLL* resonant transition in a hydrogenic ion, a summary of most of the reactions which can occur is the following:



The experiments were carried out using the 25-MV tandem accelerator of the Holifield Heavy Ion Research Facility (HHIRF) at ORNL to obtain beams of H-like  $S^{15+}$  (80–210 MeV), H-like  $Ca^{19+}$  (150–300 MeV), and He-like  $Ti^{20+}$  (237–375 MeV). The  $S^{15+}$  and  $Ca^{19+}$  ion beams were passed through the  $\langle 110 \rangle$  axis of a 1.2- $\mu\text{m}$ -thick silicon crystal. Measurements were made of (a) the emerging charge-state distributions using electrostatic deflection and a solid-state position-sensitive detector, and (b) the x-ray spectra using a Si(Li) detector with a 145 eV resolution at 5.9 keV. With this detector, we are easily able to resolve the  $h\nu_1$  ( $2p^2 \rightarrow 2p1s$ ) from  $h\nu_2$  ( $1s2p \rightarrow 1s^2$ ), but since  $h\nu_1$  and  $h\nu_3$  ( $2p \rightarrow 1s$ ) both involve decay to an empty  $K$  shell, they cannot be resolved. Hence, the experimentally distinguishable end products are  $A^{(Z-2)+}$ ,  $A^{Z+}$ , photons having energies  $h\nu_1$  and  $h\nu_3$ , and photons with energy  $h\nu_2$  (these are underlined in the above equation).

In Fig. 1(a), we show for channeled  $Ca^{19+}$  the yield of  $h\nu_1 + h\nu_3$  as a function of ion energy.<sup>5</sup> The features correspond to dielectronic excitation to  $KLL$ ,  $KLM$ ,  $KLN$ , etc., and at 300 MeV to direct  $1s \rightarrow 2p$  excitation. The energies at which these contributions should appear are indicated by the arrows at the bottom of Fig. 1(a). The magnitudes are obtained from the above rate equations, by assuming rapid substate mixing  $nl \leftrightarrow nl'$  and then using the fastest available radiative and Auger rates tabulated by Seely,<sup>6</sup> ionization cross sections calculated using the Lötzt formula,<sup>7</sup> and excitation cross sections calculated using the Seaton formula.<sup>8</sup> The collisional rates  $r_i$  are obtained from  $r_i = \sigma_i \rho_e v_i$ , where  $\rho_e$  is the electron density taken to be  $1.9 \times 10^{23} \text{ cm}^{-3}$  for the Si $\langle 110 \rangle$  channel<sup>9</sup> and  $\sigma_i$  is the cross section for the considered process.

The calculated rates are convoluted with a 10-eV Fermi distribution for the electrons in a Si $\langle 110 \rangle$  channel.<sup>9</sup> Resulting rate equations for populations of the ten lowest hydrogen- and helium-like configurations ( $1s$  to  $3l$  and  $1s^2$  to  $3l3l'$ , respectively) are iteratively solved and summation bins for numbers of x rays emitted are accumulated in 400 steps through the crystal length of 1.2  $\mu\text{m}$ . Charge-state fractions and x-ray yields per ion are calculated, including effects of Auger and x-ray decay of excited ions downstream of the crystal. The resultant  $(h\nu_1 + h\nu_3)$  x-ray yield per ion is plotted as the solid curve in Fig. 1(a). It should be noted that the only normalization is the addition of backgrounds linear in projectile energy and that the predicted values are absolute in x rays per ion. Using the same rate coefficients, we can calculate, e.g., the yield of  $Ca^{20+}$  ions [cf. Eq. (1) V(b)] and plot it together with the experimental data in Fig. 1(b).

In the case of  $Ca^{19+}$ , the radiative processes dominate, e.g., the ratio of rates for Eq. (1) III(a)/III(b)  $\approx 4$ . In the case of  $S^{15+}$ , the radiative rates are slower and the excitation and ionization cross sections are higher so that the collisional channel comes more into play; i.e., for

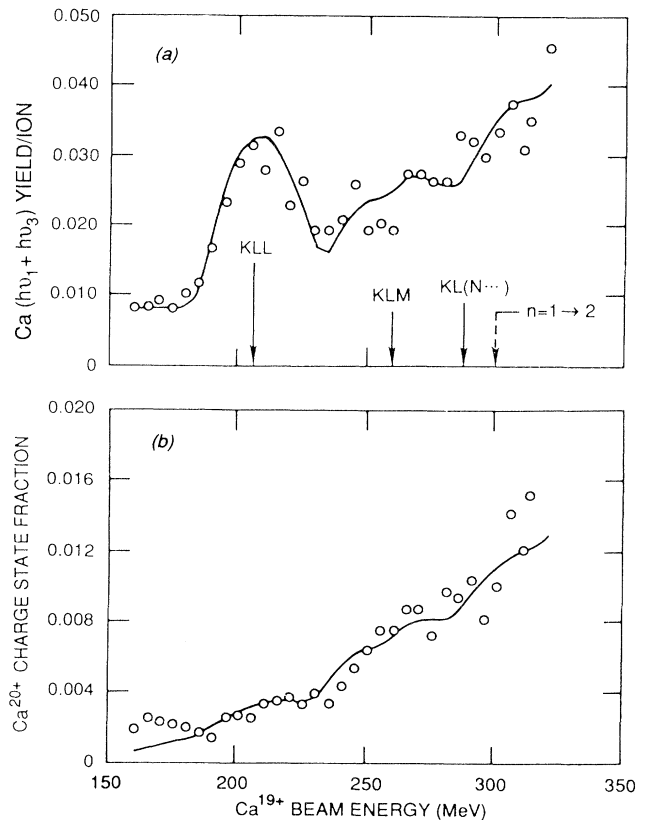


FIG. 1. (a) Yield of  $h\nu_1(2nl' \rightarrow 1snl)$  plus  $h\nu_3(2l \rightarrow 1s)$  calcium x rays [see Eq. (1)] and (b) charge fraction of  $Ca^{20+}$  ions as a function of  $Ca^{19+}$  ion energy incident on a  $\langle 110 \rangle$  channel in Si (1.2  $\mu\text{m}$  thick). The smooth curves are results of a computer simulation as described in the text.

$S^{15+}$  III(a)/III(b)  $\approx 0.8$ . In Fig. 2(a), we show, as a function of  $S^{15+}$  ion energy, the data for the yields of  $h\nu_1 + h\nu_3$  and in Fig. 2(b) the  $S^{16+}$  charge fraction. The solid curves are calculated in the same manner as for  $Ca^{19+}$  above.

The relative yields in the radiative and collisional channels can be a strong function of the crystal thickness used. The radiative rates are unaffected, but if an excited state is formed within a few mean free paths for excitation and ionization from the exit end of the crystal, the probability of it being collisionally ionized is suppressed. This is the case in the 1.2- $\mu\text{m}$  crystal used in the work described above. For example, for  $[Ca^{18+}(2p^2)]^{**}$ , the mean free path for excitation in the Si $\langle 110 \rangle$  channel is 0.72  $\mu\text{m}$  and, for the  $[S^{14+}(2p^2)]^{**}$ , the mean free path for excitation is 0.28  $\mu\text{m}$ . These effects are taken into account in our calculations. For very thin crystals (e.g.,  $< 0.05 \mu\text{m}$ ), the resulting yields should be describable in terms of simple dielectronic recombination. On the other hand, for thick crystals, only those recombined excited ions formed near the end of the path will survive while x rays formed all along the path will be recorded. We take as an example the  $KLL$  resonance in the formation of

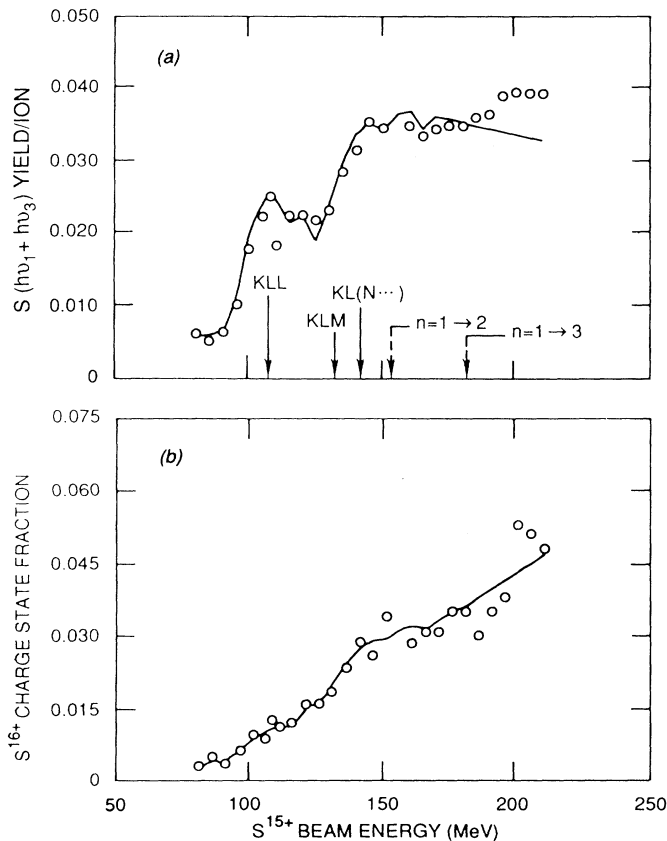
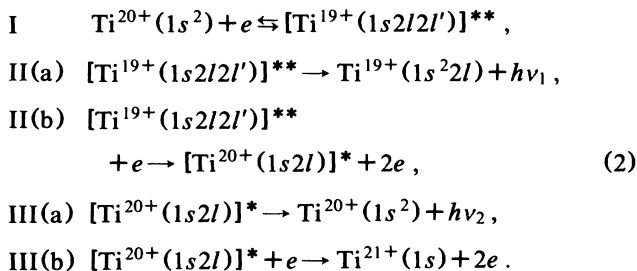


FIG. 2. (a) Yield of  $h\nu_1(2lnl' \rightarrow 1snl)$  plus  $h\nu_3(2l \rightarrow 1s)$  sulphur x rays [see Eq. (1)] and (b) charge fraction of  $S^{16+}$  ions as a function of  $S^{15+}$  ion energy incident on a  $\langle 110 \rangle$  channel in Si (1.2  $\mu\text{m}$  thick). The smooth curves are results of a computer simulation as described in the text.

Li-like Ti:



In this case, the radiative rate for II(a) exceeds the collisional rate II(b) by a factor of  $\sim 8$ . However, the stabilized recombined ion [II(a)] is susceptible to ionization via  $1s^22l + e \rightarrow 1s^2 + 3l \rightarrow 1s^2 + 2e$  with a mean free path of  $\sim 1.5 \mu\text{m}$ . We demonstrate this effect by passing a  $\text{Ti}^{20+}(1s^2)$  beam through a  $\langle 100 \rangle$  channel in a Si crystal 2.6  $\mu\text{m}$  thick.<sup>10</sup> Because of the relatively low yield of surviving  $\text{Ti}^{19+}$  ions, coincidence measurements are necessary. In Fig. 3, we show the data for coincidence of  $\text{Ti}^{19+}$  ions with Ti  $K\alpha$  and  $K\beta$  x rays. The

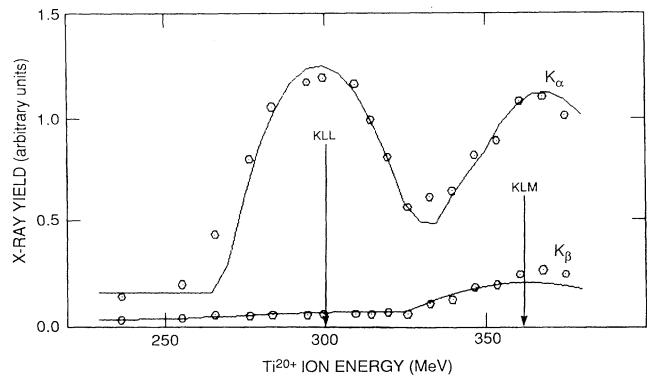


FIG. 3. Titanium  $K\alpha$  and  $K\beta$  x-ray yields for He-like ( $\text{Ti}^{20+}$ ) incident ions axially channeled through a 2.6- $\mu\text{m}$ -thick Si(100) crystal. X rays were measured in coincidence with  $\text{Ti}^{19+}$  ions. Solid curves show normalized results of a computer simulation as described in the text.

solid curves are results from a computer simulation similar to those described above for incident  $S^{15+}$  and  $\text{Ca}^{19+}$  ions. Here, electron binding and transition energies have been reduced to approximate the Li-like doubly excited states, small linear backgrounds have been added, and the calculations for  $K\alpha$  and  $K\beta$  have been independently normalized to the data at 300 MeV. Clearly, these effects should be studied as a function of path length, the upper limits being determined by complications due to the ions energy losses in the crystal.

In these experiments, we have demonstrated that a crystal channel provides an environment for electron-ion collision studies for ions with  $v_i \gg v_f$  which is quantitatively analogous to a dense electron gas with a near Fermi distribution of energies. To characterize these phenomena, we have used well understood H- and He-like ions. The utility of this work in the future lies in two directions: first, to study dielectronic excitation and collision processes of doubly excited states of more complex ions and second, to use resonances in simple ions to characterize energy distributions of electrons in crystal channels.

It is a pleasure to acknowledge J. Chevalier (Aarhus University) for his help in preparing the Si crystals. This research was sponsored by the U.S. Department of Energy, Office of Basic Energy Sciences, Division of Chemical Sciences, under Contract No. DE-AC05-84OR21400 with Martin Marietta Energy Systems, Inc.

<sup>1</sup>S. Datz, F. W. Martin, C. D. Moak, B. R. Appleton, and L. B. Bridwell, *Radiat. Eff.* **12**, 163 (1972).

<sup>2</sup>Sheldon Datz and Charles D. Moak, in *Treatise on Heavy-Ion Science*, edited by D. Allan Bromley (Plenum, New York, 1985), Vol. 6, pp. 169-240.

<sup>3</sup>S. Andriamonje, M. Chevallier, C. Cohen, J. Dural, M. J.

Gaillard, R. Genre, M. Hage-Ali, R. Kirsch, A. L'Hoir, B. Mazuy, J. Mory, J. Moulin, J. C. Poizat, J. Remillieux, D. Schmaus, and M. Toulemonde, *Phys. Rev. Lett.* **59**, 2271 (1987).

<sup>4</sup>N. Claytor, B. Feinberg, H. Gould, C. E. Bemis, Jr., J. Gomez del Campo, C. A. Ludemann, and C. R. Vane, *Phys. Rev. Lett.* **61**, 2081 (1988).

<sup>5</sup>Tests of the channeling effect on charge states and x rays were duly carried out. For example, 315-MeV  $\text{Ti}^{20+}$ ,  $\text{Ti}^{21+}$ , and  $\text{Ti}^{22+}$  beams injected in a random direction all resulted in the same (equilibrium) exit charge-state distribution ( $18+ = 6\%$ ,  $19+ = 18\%$ ,  $20+ = 40\%$ ,  $21+ = 30\%$ , and  $22+ = 6\%$ ), while the same beams injected in a channeling direction resulted in exit charges fractions which had  $> 85\%$  in the entering charge state.

<sup>6</sup>J. F. Seely, *At. Data Nucl. Data Tables* **26**, 137 (1981).

<sup>7</sup>W. Lötzer, *Z. Phys.* **206**, 206 (1968); R. A. Phaneuf, in *Atomic Processes in Electron-Ion and Ion-Atom Collisions*, edited by F. Brouillard (Plenum, New York, 1986), p. 139, Eq. 3.7.

<sup>8</sup>M. J. Seaton, in *Atomic and Molecular Processes*, edited by D. R. Bates (Academic, New York, 1962), p. 374.

<sup>9</sup>B. R. Appleton, R. H. Ritchie, J. A. Biggerstaff, T. S. Noggle, S. Datz, C. D. Moak, H. Verbeek, and V. N. Neelavathi, *Phys. Rev. B* **19**, 4347 (1979); see discussion on p. 4356.

<sup>10</sup>The incident beam is expected to be essentially pure ground state as the flight time from the stripper foil is approximately 20 times the metastable  $1s2s(^3S_1)$   $M1$  lifetime (26 nsec); see H. Gould, R. Marrus, and P. J. Mohr, *Phys. Rev. Lett.* **31**, 504 (1973).